Modeling of the Sulfidation of Zinc-Titanium Oxide Sorbents with Hydrogen Sulfide

Susan Lew, Adel F. Sarofim, and Maria Flytzani-Stephanopoulos
Dept. of Chemical Engineering, Massachusetts Institute of Technology, Cambridge, MA 02139

The overlapping grain model was used to describe the sulfidation of zinc oxide and zinc-titanium oxide powders at temperatures between 400–700°C in H_2S-H_2-N_2 gas mixtures. Experimental data were collected under conditions free of mass-transfer and pore diffusion limitations. Thus, the only resistances to reaction were due to intrinsic sulfidation kinetics (surface reaction) and diffusion through the product layer. The product layer diffusion coefficient was used as a fitting parameter in the model. As the relative amount of titanium in the sorbent was increased, the product layer diffusion coefficient decreased. Similar activation energies (26.6 kcal/mol) were obtained for the product layer diffusion coefficient of ZnO and Zn-Ti-O sulfidation. From the similarity in activation energies, it is proposed that for both types of sorbents diffusion occurs primarily through ZnS.

Introduction

The gas-solid reaction of hydrogen sulfide with metal oxides is of interest in connection with developing regenerable oxide sorbents for hot coal gas desulfurization. Direct removal of H_2S from the hot fuel gas can significantly improve the thermal efficiency of emerging technologies using coal gasification such as integrated gasification combined-cycle power generation and gasifier-molten carbonate fuel cells (Marqueen et al., 1986). Hot gas cleanup will also eliminate the costs of heat exchangers to cool down the fuel gas, reheating equipment, and expensive waste water cleanup processes, which put the commercial (low-temperature) H_2S removal processes at a disadvantage. Various metal oxide sorbents have been considered for high-temperature H_2S removal (MERC, 1978). Among them, zinc oxide is attractive because it combines good sulfidation equilibria, fast kinetics and regenerability. Over the past decade, zinc oxide neat or in combination with iron oxide has been studied for hot gas cleanup applications (Grindley and Steinfeld, 1981; Tamhankar et al., 1986; Focht et al., 1988). A major limitation of ZnO-based sorbents for hot gas desulfurization is sorbent loss due to the reduction of zinc oxide to volatile elemental zinc. We have found that zinc-titanium-oxide solids are much more resistive to reduction by H_2 than ZnO (Lew, 1990; Lew et al., 1989; 1992a). The initial sulfidation rate of Zn-Ti-O solids was approximately half that of ZnO (Lew, 1990; Lew et al., 1992b). In this article, we examine the product layer diffusion in Zn-Ti-O sulfidation. Comparison with ZnO sulfidation will be made.

A reaction model is used to describe the influence of different resistances (for example, mass transfer, pore diffusion, chemical reaction and product layer diffusion resistances) on the conversion-time profile. Gibson and Harrison (1980) and Ranade and Harrison (1981) used the grain model to describe the ZnO-H_2S reaction system. In this model, the solid is described as an assemblage of nonoverlapping grains reacting independently of each other. Each grain can be regarded as a shrinking nonporous reactant core. Around each grain, reaction with H_2S produces a nonporous sulfide product layer.

Recently, as it became evident that the grain model inadequately describes many solid structures, modifications were made. One weakness of the grain model lies in the assumption that the solid is composed of nonoverlapping grains where the individual grains grow independently with no overlapping of the product layer. To provide a more realistic description of the solid, Lindner and Simonsson (1981) represented the initial solid structure as an aggregate of truncated spheres (that is, overlapping spheres) in contact with each other in an initial stage of sintering. Sotirchos and Yu (1988) further refined this overlapping grain model by representing the solid as an assemblage of grains randomly placed in space with overlapping of the grains possible.

The overlapping grain model is more flexible and powerful than the grain model in that it can predict various behaviors (for example, a maximum in the rate-conversion profile). The

Correspondence concerning this article should be addressed to M. Flytzani-Stephanopoulos.
Present address of S. Lew: ARCO Chemicals Co., Newtown Square, PA 19073

Table 1. Physical and Chemical Properties of Solids Used in Sulfidation Experiments*

Sorbent	$(Zn/Ti)_{atomic}$	Surface area (m^2/g)	Pore** Vol (cm^3/g)	Crystalline Phase (wt. %)
ZnO†	--	2.4	1.20	ZnO (100)
Z2T-a	2/1	4.1	0.73	Zn_2TiO_4 (100)
Z2T-b‡	2/1	13.9	1.13	Zn_2TiO_4 (100)
Z2T3	2/3	2.3	0.47	$ZnTiO_3$(65), $Zn_2Ti_3O_8$ (16), TiO_2 (19)

* Prepared from zinc acetate and titanium (IV) i-propoxide with 1:1 mole ratio of metal ions to citric acid. Calcined at 720°C for 12 h.
** Particle size: 90-125 μm.
† Calcined at 720°C for 4 h.
‡ Prepared with 1:2 mole ratio of metal ions to citric acid.

grain model predicts a monotonically decreasing reaction surface area with conversion and the anomaly of a monotonically increasing pore surface area even when the porosity reduces to zero (Szekely et al., 1976). However, as with all models which try to approximate realistic behavior closely, the computational complexity of the random overlapping grain model is greater than that of the grain model.

We have recently conducted an extensive experimental study of the sulfidation kinetics of Zn-Ti-O and ZnO sorbents with H_2S-H_2O-H_2-N_2 gas mixtures in a thermogravimetric apparatus (Lew, 1990; Lew et al., 1991; 1992b). The scanning electron micrographs of these solids show a consistent picture of overlapping grains. At high sulfidation conversions overlapping of the product layer was seen. Based on the SEM pictures, the overlapping grain model of Sotirchos and Yu (1988) was used to describe the solids. This model was used to determine the effect of titanium content of the sorbents on the product layer diffusion rate.

Experimental Methods

In the sulfidation experiments discussed in Lew (1990) and Lew et al. (1991; 1992b), macroporous solid powders were reacted with H_2S. Bulk mixed oxide solids of zinc and titanium were prepared for the sulfidation experiments by a known method for synthesizing highly dispersed mixed oxides from amorphous citrate precursors (Marcilly et al., 1970; Courty et al., 1973). Preparations are discussed in more detail in Lew (1990) and Lew et al. (1990; 1991b).

The solids were characterized by several bulk and surface analysis techniques. Table 1 lists the properties of the solids discussed in this paper. The elemental composition (zinc and titanium) of the solids was verified by atomic absorption spectroscopy (Perkin Elmer Spectrophotometer) of the solids dissolved in a hot HF-HCl-H_2O solution (approximately 90°C). X-ray diffraction (XRD) for identification of crystalline phases in the mixed oxides was performed with a Rigaku RU300 instrument using Cu(Kα) radiation. Scanning electron microscopy (SEM) using a Cambridge Stereoscan 250 MK3 instrument was used to observe the surface morphology and crystallite size of the solids. Surface areas were measured by a Micromeritics Flow Sorb III 2300 BET apparatus using N_2 gas while pore volumes and pore size distribution were measured by a Micromeritics Autopore 9200 mercury porosimeter.

Experiments of sulfidation kinetics of solids containing various Zn/Ti atomic ratios were performed in a Cahn System 113-X thermogravimetric analyzer (TGA) equipped with a Cahn 2000 electrobalance, a Micricon temperature controller, and a Bascom Turner data acquisition system. The TGA measured the weight gain as a function of the time required for Zn-Ti oxides sulfidation to ZnS and TiO_2. The solids were pretreated in a vacuum oven at 90°C for 1 h to remove any adsorbed H_2O before they were reacted in the TGA.

To eliminate mass-transfer limitations, sample quantity was decreased and gas flowrate was increased until variation in either of these parameters showed no effect on the reaction profile. Pore diffusion limitation was eliminated by decreasing the particle size until no effect on the reaction profile was observed. With the macroporous particles used here, particle size of 90-125 μm was found adequately small for all solids except *Z2T-a*, for which 43-65 μm size particles were used. A thin layer of sample (typically 1-3 mg of 90-125 μm size particles) was placed in a hemispherical quartz pan suspended by a quartz hangdown wire. Thus, the measured rate was due only to intrinsic sulfidation kinetics and product layer diffusion.

The Overlapping Grain Model

The gas-solid sulfidation reaction can be represented by the general stoichiometry:

$$A(g) + bB(s) \rightarrow cC(g) + dD(s) \tag{1}$$

The porous solid is simulated as an assemblage of grains randomly distributed in space. The centers of the grains are randomly placed in space with overlapping of the grains permitted. This is consistent with the observed solid structures of the sorbents in this study. If the solid product occupies more volume than a stoichiometrically equal volume of reactant, as it does in this study (for example, for ZnO sulfidation: molar volume of product/molar volume of reactant, $Z = 1.64$), then overlapping of the product resulting in pore closure is possible.

In this model (Sotirchos and Yu, 1988), the porosity ϵ and surface area S of the reaction r and pore p surface at time t are defined as:

$$\epsilon_r = \exp\left[-f \int_{Y(t)}^{r_{o,\max}} r_r^{F_g} n_o(r_o) dr_o \right] \tag{2}$$

$$S_r = F_g f \epsilon_r \int_{Y(t)}^{r_{o,\max}} r_r^{F_g - 1} n_o(r_o) dr_o \tag{3}$$

$$\epsilon_p = \exp\left[-f \int_{r_{o,\min}}^{r_{o,\max}} r_p^{F_g} n_o(r_o) dr_o \right] \tag{4}$$

$$S_p = F_g f \epsilon_p \int_{r_{o,\min}}^{r_{o,\max}} r_p^{F_g - 1} n_o(r_o) dr_o \tag{5}$$

where F_g is the grain shape factor (sphere = 3; cylinder = 2, plate = 1); r_o is the initial radius; f is the grain geometric factor (sphere = $4\pi/3$; cylinder = πL_{avg}; plate = $2A_{avg}$), L_{avg} and A_{avg} are the average grain length of the cylinder and the average grain surface area of plate-like grain, respectively; $n_o(r_o)dr_o$

is the number of grains per unit volume with radius in the initial size range $[r_o, r_o+dr_o]$; $r_{o,\min}$ and $r_{o,\max}$ are the initial lower and upper grain radius limit; $Y(t)$ is the lower active reactant grain radius limit. The pore surface makes up the sum of the solid reactant and the product. Thus, the pore surface is equivalent to the reactant surface when the reaction time is zero.

The structural expressions (Eqs. 2-5) can be incorporated into a rate expression to yield:

$$\frac{dr_r}{dt}=\frac{\dfrac{-bkC_{Ao}}{\rho_s}}{1-\dfrac{k}{D_e}\epsilon_r r_r^{F_g-1}\displaystyle\int_{r_p}^{r_r}\frac{dr}{\epsilon(t')r^{F_g-1}}} \tag{6}$$

where k is the rate constant; D_e is the product layer diffusion coefficient; C_{Ao} is the concentration of A (that is, H_2S) in the bulk gas; ρ_s is the molar concentration of solid B, ϵ is the porosity. At r_p, $\epsilon=\epsilon_p$ and at r_r, $\epsilon=\epsilon_r$. The change in the pore radius r_p is related to reaction surface radius r_r by

$$\frac{dr_p}{dt}=-\frac{dr_r}{dt}\left[(Z-1)\frac{\epsilon_r r_r^{F_g-1}}{\epsilon_p r_p^{F_g-1}}\right] \tag{7}$$

The porosity of the solid (product + reactant) is found by

$$\epsilon_p=\epsilon_o-(Z-1)(\epsilon_r-\epsilon_o) \tag{8}$$

The fractional conversion is calculated with

$$X=\frac{\epsilon_o-\epsilon_p}{(Z-1)(1-\epsilon_o)} \tag{9}$$

Equations 6-9 were used to evaluate the experimental results obtained for sulfidation of ZnO and Zn-Ti-O sorbents. The rate constant k was obtained from initial rate measurements (Lew, 1990; Lew et al., 1992b). The sulfidation profile predicted with the overlapping grain model was fitted to the experimental sulfidation profile by using the effective product layer diffusion coefficient D_e as a fitted parameter.

Table 2. Parameter Values Used to Calculate the ZnO Sulfidation Profiles

ϵ_o (Porosity)	0.59
r_o (Grain Radius, cm)	1.6×10^{-5}
ρ_s (Density, mmol/cm^3)	68.9
k (Rate Constant, cm/s)	1.3exp[−10.3 kcal/mol/RT]
Molar Gas Composition	2% H_2S-1% H_2-97% N_2
Z	1.64
D_e (cm^2/s), 400°C	2.7×10^{-10}
500°C	3.0×10^{-9}
600°C	2.0×10^{-8}
700°C	1.0×10^{-7}

Application to ZnO and Zn-Ti-O Sulfidation

For ZnO, based on SEM micrographs (for example, Figure 1), a uniform size of spherical grains was used in the overlapping grain model. Table 2 lists the values of the physical properties of ZnO used in this model. The overall sulfidation reaction is

$$H_2S(g)+ZnO(s)\rightarrow H_2O(g)+ZnS(s) \tag{10}$$

The initial grain radius based on randomly overlapping spherical grains is defined as:

$$r_o=-\frac{3\epsilon_o}{S_o}\ln\epsilon_o \tag{11}$$

Values for S_o were obtained from BET measurement. ϵ_o values were obtained from mercury porosimetry. The calculated initial grain radius from Eq. 11 was 0.16 μm for ZnO. This was closer to the actual grain size seen in SEM micrographs (for example, Figure 1) than the value predicted by the grain model (0.22 μm). The grain size distribution shown in Figure 2 was measured from SEM micrographs of ZnO. A comparison of the predicted reaction profiles with the experimental reaction profiles obtained with 2% H_2S-1% H_2-97% N_2 at temperatures of 400-700°C is shown in Figure 3. The values of the effective product layer diffusion coefficients used in the calculation are listed in Table 2. As shown in Figure 3, the predicted and the

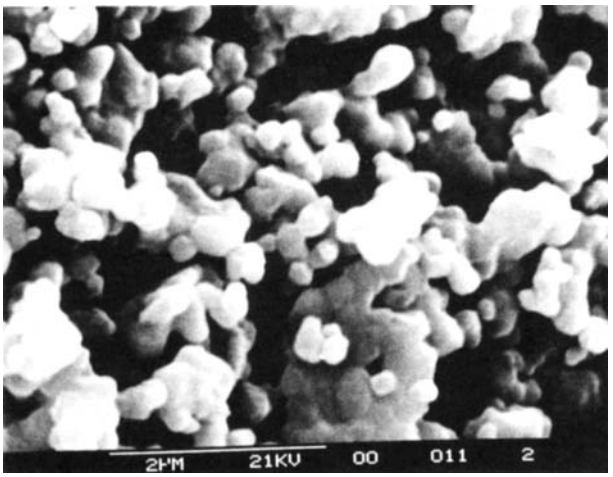

Figure 1. SEM micrograph of ZnO calcined at 720°C for 4 h showing overlapping spherical grains.

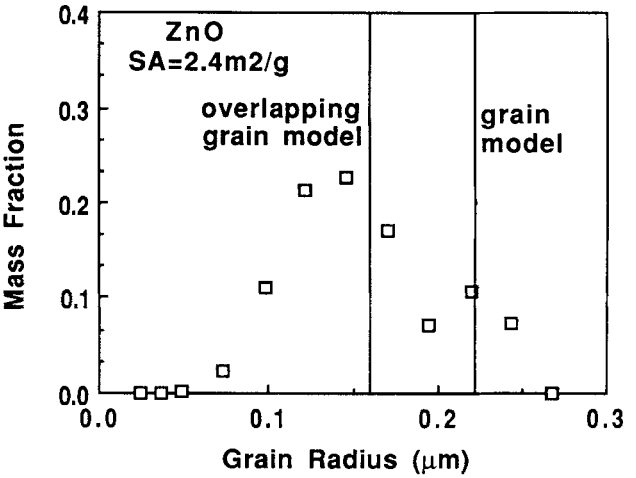

Figure 2. Grain size distribution of ZnO calcined at 720°C for 4 h.

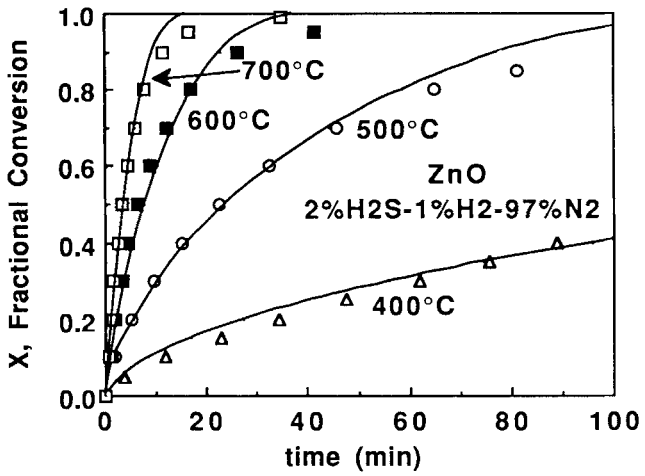

Figure 3. Experimental sulfidation profiles of ZnO at 400-700°C (2% H_2S-1% H_2-97% N_2) vs. calculated profiles from overlapping grain model.

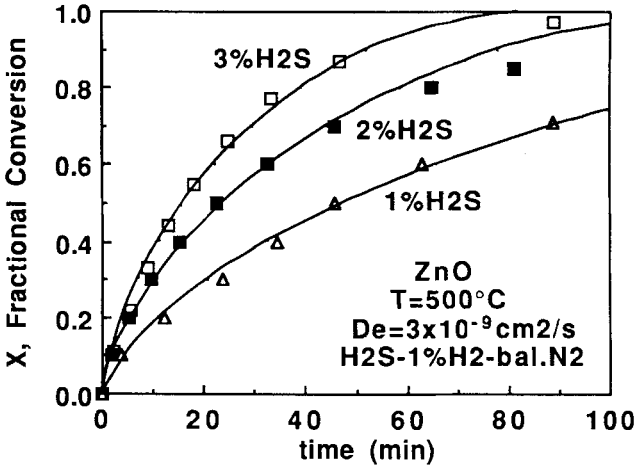

Figure 5. Experimental sulfidation profiles of ZnO at 500°C reacted in 1, 2 and 3% H_2S vs. calculated profiles from overlapping grain model.

experimental profiles are in good agreement. There was also good agreement between the predicted surface area and the measured surface area at different extent of sulfidation as shown in Figure 4. This figure also shows the predicted surface area when using a nonoverlapping grain model.

The predicted sulfidation profiles using the value of D_e calculated from the experiments performed with 2% H_2S-1% H_2-97% N_2 are consistent with the experimental profiles obtained with various H_2S concentrations as shown in Figure 5. Consequently, the assumption in Eq. 6 that the H_2S bulk concentration is equal (or proportional) to the concentration of the rate-limiting diffusing species in the product layer is correct.

The overlapping grain model was applied to the sulfidation of Zn-Ti-O sorbents. The overall reaction is:

$$H_2S(g) + 1/x Zn_xTi_yO_{x+2y}(s) \rightarrow H_2O(g) + ZnS(s) + y/x TiO_2(s) \quad (12)$$

Based on SEM micrographs of Zn-Ti-O solids, such as Figure 6 for sorbent *Z2T-a* (*2Zn*:1*Ti*), the solids typically consist of grains of various sizes. For the modeling, the solid structure was simplified by considering only two discrete grain sizes (that is, a discrete bimodal grain size distribution). The sizes of these grains were estimated using the SEM micrographs of the unreacted sorbents. The relative mass fraction of each type of grains was estimated using the surface area, porosity, and pore-size distribution information for the solids. The modeling of sorbents *Z2T-a* (*2Zn*:1*Ti*) and *Z2T3-a* (*2Zn*:3*Ti*) will be discussed. Three possible Zn-Ti-O phases are found in these solids, $Zn_2Ti_3O_8$, Zn_2TiO_4 and $ZnTiO_3$. From our sulfidation kinetic experiments, they were found to have approximately the same chemical sulfidation rate (Lew, 1990; Lew et al., 1992b). Modeling of other Zn-Ti-O sorbents used the same method.

Sorbent *Z2T-a* consisted of two types of grains. One type

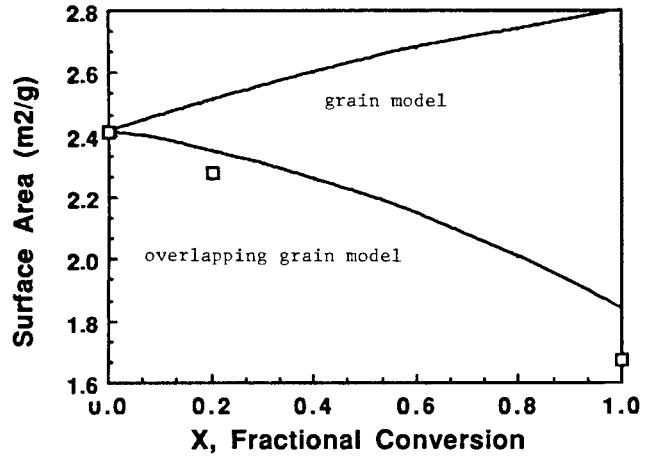

Figure 4. Surface area variation predicted by the random overlapping grain model vs. the grain model with experimental results (□) of ZnO sulfidation at 650°C (2% H_2S-1% H_2-97% N_2).

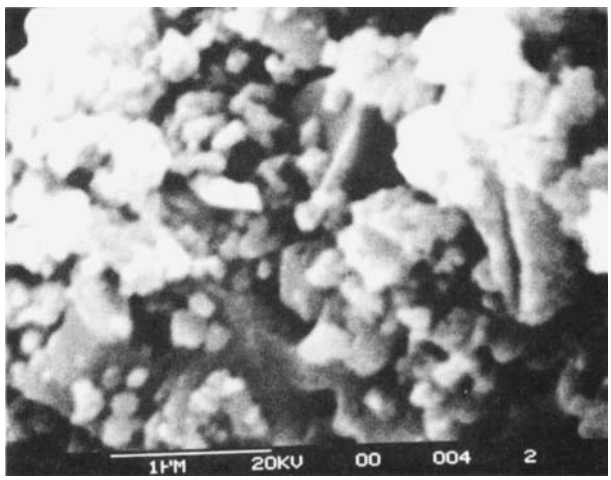

Figure 6. SEM micrograph of *Z2T-a* calcined at 720°C for 12 h showing nonuniform grain size distribution.

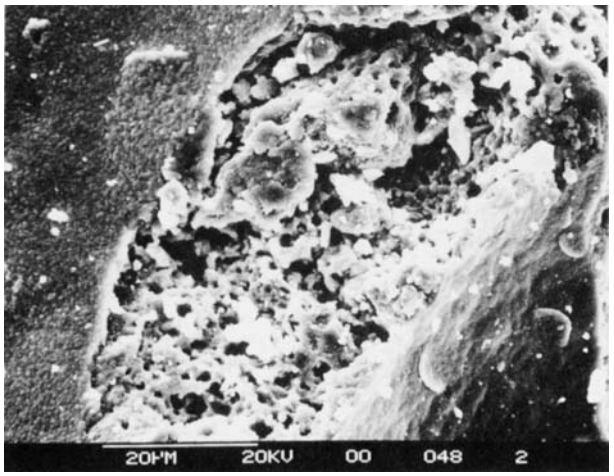

Figure 7. SEM micrograph of 90% sulfided *Z2T-a* at 650°C in 2% H_2S-1% H_2-97% N_2.

Interior: S/Zn = 1.0 and "skin":S/Zn = 0.7.

was small spherical grains approximately 0.05 μm in radius. The other was flat plate-like grains. These plate-like grains measured approximately 0.2 μm (half-thickness). A rough estimate of the relative mass percentage of the two grain types finds approximately a 50%-50% distribution. For the modeling, it was assumed that there was no interaction between the two types of grains (that is, no overlapping of products originating from two different grain types). Based on SEM micrographs of Zn-Ti-O solids, this is a good assumption. For plate-like grains, the initial grain radius (that is, half-thickness) is

$$r_o = -\frac{\epsilon_o}{S_o} \ln \epsilon_o \tag{13}$$

These greatly different grain sizes result from the amorphous citrate technique used in preparation of the Zn-Ti-O solids. Zinc titanates prepared by the amorphous citrate technique form a "skin" of low porosity. In comparison with this "skin", the rest of the solid is composed of smaller spherical overlapping grains. The Zn-Ti-O solids "skin" formation causes lower solid reactivity in sulfidation. This is shown in Figure 7 for *Z2T-a* which was approximately 90% sulfided. The "skin" of the solid (left side of Figure 7) contained $(S/Zn)_{\text{atomic ratio}} = 0.7$ while the center portion of the figure contained $(S/Zn)_{\text{atomic ratio}} = 1.0$.

A comparison of the predicted profiles from the overlapping grain model and the experimental sulfidation profiles for *Z2T-a* is shown in Figure 8. Figure 8a shows the experimental and predicted reaction profiles at 500°C. The individual contributions that the spherical grains and plate-shaped grains make to the overall conversion profile are also shown in Figure 8a. The overall predicted conversion profiles at various other temperatures are shown in Figure 8b. The parameter values used to calculate the profiles in Figure 8 are listed in Table 3. A verification of the improvement obtained by using a discrete bimodal grain size distribution for the modeling of *Z2T-a* was the agreement between the effective diffusion coefficient predicted from the reaction profiles of *Z2T-a* and *Z2T-b*. These

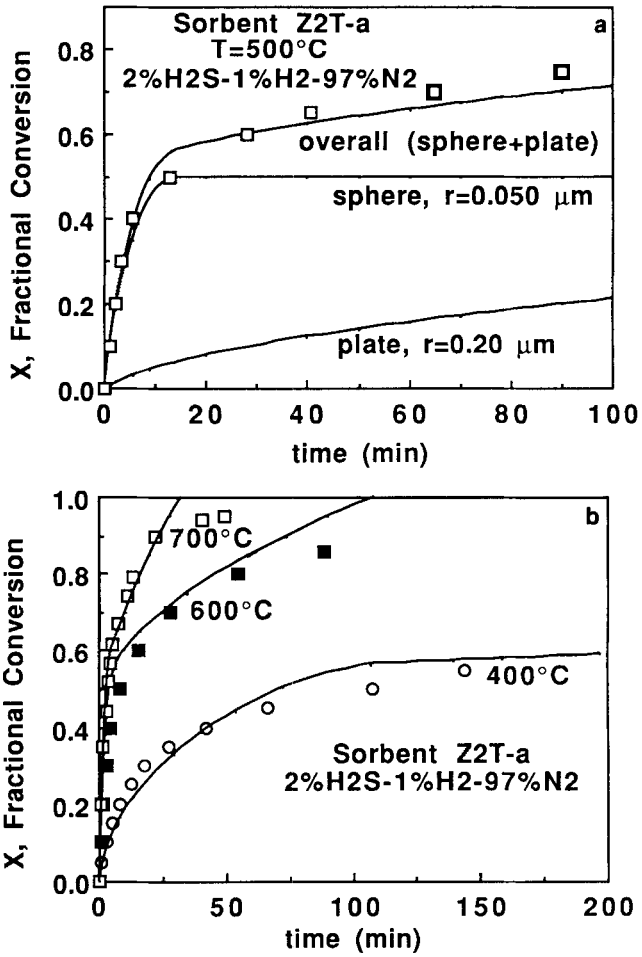

Figure 8. Experimental sulfidation profiles of *Z2T-a* vs. calculated profiles from overlapping grain model with a discrete bimodal grain-size distribution at (a) 500°C and (b) various other temperatures.

two solids have the same chemical phases, but have different physical properties (See Table 1). In contrast to *Z2T-a*, a uniform grain structure was present in *Z2T-b*. At 400°C, the calculated effective diffusion coefficient for *Z2T-a* was

Table 3. Parameter Values Used to Calculate the *Z2T-a* Sulfidation Profiles

ρ_s (Density, mmol/cm^3)	21.8
k (Rate Constant, cm/s)	0.40exp[−9.3 kcal/mol/RT]
Molar Gas Composition	2% H_2S-1% H_2-97% N_2
Z	1.45
b	0.5
D_e (cm^2/s), 400°C	1.8×10^{-10}
500°C	2.2×10^{-9}
600°C	1.3×10^{-8}
700°C	8.3×10^{-8}
Sphere Grains (50 wt. %)	
ϵ_o (Porosity)	0.42
r_o (Grain Radius, cm)	5×10^{-6}
Plate-Like Grains (50 wt. %)	
ϵ_o (Porosity)	0.72
r_o (Grain Radius, cm)	2×10^{-5}

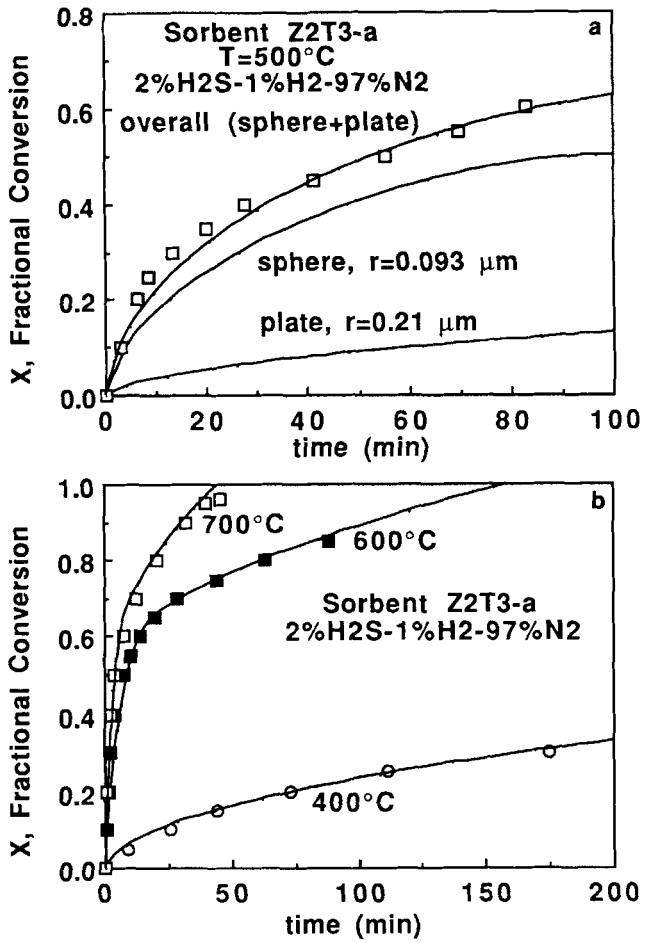

Figure 9. Experimental sulfidation profiles of *Z2T3-a* vs. calculated profiles from the overlapping grain model with a discrete bimodal grain size distribution at (a) 500°C and (b) various other temperatures.

1.8×10^{-10} cm^2/s while for *Z2T-b*, a value of 1.5×10^{-10} cm^2/s was calculated. Similar agreement between the predicted and experimental reaction profiles was obtained for sorbent *Z2T3-a* using a bimodal grain size distribution in the overlapping grain model as shown in Figure 9. The values used to calculate the profiles in Figure 9 are listed in Table 4.

Table 4. Parameter Values Used to Calculate the *Z2T3-a* Sulfidation Profiles

ρ_s (Density, mmol/cm^3)	11.7
k(Rate Constant, cm/s)	0.40exp[−9.3 kcal/mol/RT]
Molar Gas Composition	2% H_2S-1% H_2-97% N_2
Z	1.22
b	0.5
D_e (cm^2/s), 400°C	3.5×10^{-11}
500°C	4.2×10^{-10}
600°C	3.6×10^{-9}
Spherical Grains (50 wt. %)	
ϵ_o (Porosity)	0.42
r_o (Grain Radius, cm)	9×10^{-6}
Plate-Like Grains (50 wt. %)	
ϵ_o (Porosity)	0.81
r_o (Grain Radius, cm)	2×10^{-5}

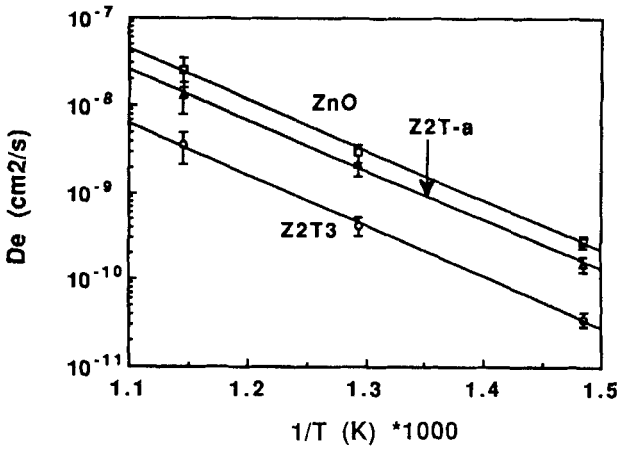

Figure 10. Arrhenius plots of the product layer diffusion coefficients for various sorbents.

Effect of TiO_2 on the Product Layer Diffusion

The calculated effective diffusion coefficient using the overlapping grain model for the sulfidation of Zn-Ti-O sorbents of various compositions indicated a dependence on the relative amount of titanium in the sorbents. The diffusion coefficient can be represented by the Arrhenius law as follows

$$D_e = D_{e,o}\exp(-E/RT) \tag{14}$$

where the preexponential factor ($D_{e,o}$) and the activation energy (E) are not temperature dependent. An Arrhenius plot of the experimentally calculated diffusion coefficients for sorbents ZnO, *Z2T-a*, and *Z2T3-a* is shown in Figure 10. Table 5 lists the calculated Arrhenius constants. The Arrhenius plot of the diffusion coefficient is shown for temperatures up to 600°C. At higher temperatures, the relative resistance of the chemical reaction becomes more dominant compared to the diffusional resistance because of the higher activation energy of the product layer diffusion coefficient (26.6 kcal/mol) compared to that of the chemical reaction rate constant (9–10 kcal/mol). The relative importance of the product layer and chemical reaction resistances is a function of the product layer diffusion coefficient, chemical rate constant, temperature, and grain size. For smaller grain sizes, the product layer diffusion resistance decreases because of the smaller corresponding product layer diffusion lengths involved.

Similar activation energies (26.6±0.3 kcal/mol) were obtained for ZnO and Zn-Ti oxides. The major difference is in the pre-exponential factor. Sorbents with increasing relative

Table 5. Arrhenius Constants for the Product Layer Diffusion Coefficient (D_e)

Sorbent	Temp. (°C)	Arrhenius Constants $D_{e,o}$, cm^2/s	E, kcal/mol
ZnO	400–600	0.098	26.4
Z2T-a	400–600	0.053	26.3
Z2T3-a	400–600	0.019	27.0

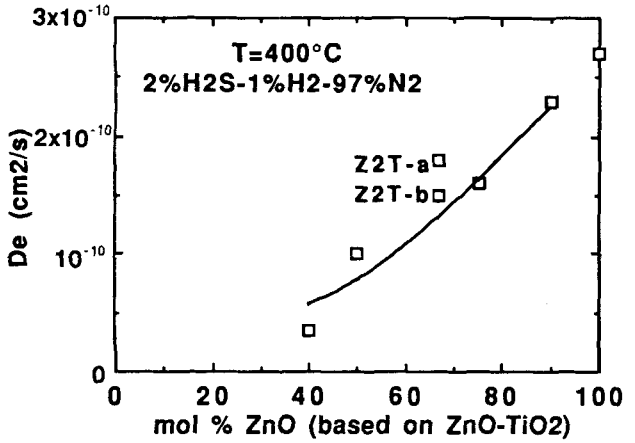

Figure 11. Comparison of predicted and experimental product layer diffusion coefficients for various Zn-Ti-O sorbents sulfided at 400°C.

concentration of titanium have correspondingly decreasing preexponential factor. The high activation energy is consistent with diffusion by a solid state mechanism. The similarity in activation energies suggests that in a product layer containing a mixture of ZnS and TiO_2 diffusion occurs through ZnS and not through TiO_2. Diffusion preferentially occurs through the fastest pathway. The role of TiO_2 is to decrease the cross-sectional area available for diffusion and increase the tortuosity of the diffusion pathway. The change in the diffusion coefficient can be mathematically expressed by adapting the equation for the "random pore" model proposed by Wakao and Smith (1962) for diffusion in a porous solid having a bimodal pore-size distribution separated into macropores and micropores:

$$D_e = \epsilon_m^2 D_{e,m} + \left[\frac{\epsilon_\mu^2(1+3\epsilon_m)}{(1-\epsilon_m)}\right] D_{e,\mu} \tag{15}$$

where ϵ_m and ϵ_μ are the macroporosity and microporosity, respectively. $D_{e,m}$ and $D_{e,\mu}$ are the diffusion coefficients. For this system, a similar expression as Eq. 15 is used with the porosities replaced by the volume fractions (ν) of ZnS and TiO_2:

$$D_{e,\mathrm{ZnS+TiO_2}} = \nu_{\mathrm{ZnS}}^2 D_{e,\mathrm{ZnS}} + \left[\frac{\nu_{\mathrm{TiO_2}}^2(1+3\nu_{\mathrm{ZnS}})}{(1-\nu_{\mathrm{ZnS}})}\right] D_{e,\mathrm{TiO_2}} \tag{16}$$

The diffusion flux in the product layer is the sum of that through ZnS, that through TiO_2, and that through ZnS and TiO_2 in series. For $D_{e,\mathrm{ZnS}} \gg D_{e,\mathrm{TiO2}}$, this reduces to:

$$D_{e,\mathrm{ZnS+TiO_2}} = \nu_{\mathrm{ZnS}}^2 D_{e,\mathrm{ZnS}} \tag{17}$$

Equation 17 is used to predict the product layer diffusion coefficient for various Zn-Ti oxides sulfided at 400°C. The value of $D_{e,\mathrm{ZnS}}$ was obtained from ZnO sulfidation results. As shown in Figure 11, the agreement between the experimental and predicted values is good.

The measured product layer diffusion coefficient for ZnO sulfidation in this work is higher than values reported in earlier literature. Ranade and Harrison (1980) reported an activation energy of 22 kcal/mol and a preexponential factor of 4.9×10^{-4} cm^2/s for the product layer diffusion coefficient in ZnO sulfidation. For ZnO, an activation energy of 26.4 kcal/mol and a preexponential factor of 0.098 cm^2/s were found in this study. At 600°C, the diffusion coefficient measured in this study was 14 times higher than that measured by Ranade and Harrison. The reason for this difference is not clear. However, the ZnO solid used by Ranade and Harrison was only 94.5% pure. It is not known how the unspecified impurity may have affected the product layer diffusion.

The large value of the activation energy (26.6 ± 0.3 kcal/mol) of the diffusion coefficient implies ionic diffusion through a solid nonporous product layer. The possible rate-limiting diffusing species in the product layer are Zn and OH ions diffusing out to the gas phase and S and H ions diffusing into the unreacted core. In addition, there is the possibility of electron diffusion to maintain the charge balance. Diffusion of H^+ is very fast. At the gas-solid interface, OH^- ions are consumed by the reaction:

$$OH^- + H^+ = H_2O \tag{18}$$

The presence of H_2O in the gas increases the amount of OH^- ions at the gas-solid interface, thus, decreasing the diffusion rate of OH^- ions out of the solid. However, when H_2O was added to the gas stream, no change in the product layer diffusion coefficient was observed.

The addition of H_2 will increase the Zn^{2+} at the reactant-product interface by the reaction:

$$ZnO + H^+ = Zn^{2+} + OH^- \tag{19}$$

Thus, this can change the diffusion rate of Zn cations. However, again no change in the product layer diffusion coefficient was observed for various H_2 concentrations. Thus, the probable diffusion limiting species is S^{2-}. The calculation of D_e was based on a gaseous concentration gradient ($C_{\mathrm{H_2S},o} - C_{\mathrm{H_2S},s}$). Since S^{2-} ions are diffusing, an ionic concentration gradient must be used. As shown in Figure 5, when the H_2S concentration is varied, it is not necessary also to vary the product layer diffusion coefficient to fit the data. Based on this observation and since the initial sulfidation reaction rate is first-order, the chemisorption of H_2S on the solid is a first-order process with

$$C_{S^{2-},o} = K_{\mathrm{H_2S}} C_{\mathrm{H_2S},o} \tag{20}$$

where $K_{\mathrm{H_2S}}$ is the adsorption equilibrium constant of H_2S, and $C_{\mathrm{H_2S},o}$ is the bulk H_2S concentration. Thus the rate expression (Eq. 6) becomes

$$\frac{dr_r}{dt} = \frac{\dfrac{-bkK_{\mathrm{H_2S}} C_{\mathrm{H_2S},o}}{\rho_s}}{1 - \dfrac{k}{D_e} S_r \displaystyle\int_{r_p}^{r_r} \frac{dr}{S}} \tag{21}$$

With the limitation in scope of this study, it was not possible to determine $K_{\mathrm{H_2S}}$, which was arbitrarily set equal to unity. Thus, comparison with the diffusion coefficient from other

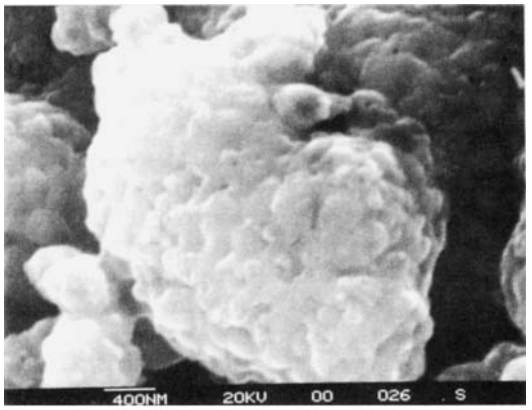

(a)

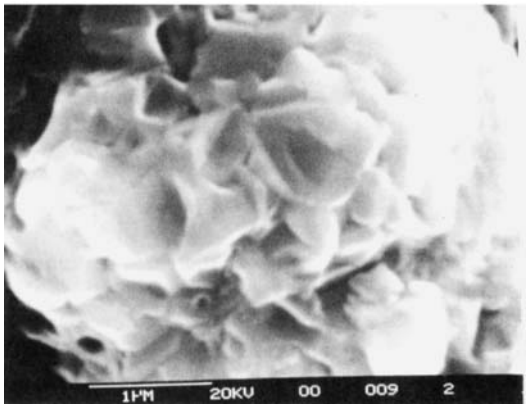

(b)

Figure 12. SEM micrographs of solids sulfided at 600°C with 2% H_2S-1% H_2-97% N_2: (a) ZnO and (b) *Z2T-a*.

studies must keep in mind that differences in values may be attributed to the value used for the driving force of diffusion. Secco (1958) measured the diffusion of Zn cations in ZnS crystals by a radiotracer technique. An activation energy of 35 kcal/mol and preexponential factor of 3×10^{-4} cm^2/s were reported. No values for S anion diffusion coefficient are available, but it is expected to be smaller since the ionic radius of S^{2-} is 2.45 times larger than Zn^{2+} (Shannon and Prewitt, 1969). In any case, this diffusion coefficient is much smaller than the values obtained here for the sulfidation of ZnO. Differences in the measured values of the diffusion coefficient can also be attributed to different mechanisms. Secco (1958) measured lattice diffusion while in this study diffusion via grain boundaries, which is characterized by faster diffusion rate and lower activation energy for the diffusion coefficient (Kingery et al., 1976), is believed to be dominant. Grain boundaries are apparent in both sulfided ZnO and *Z2T* (Figure 12).

Summary

The overlapping grain model which allows for randomly overlapping grains was used to predict the sulfidation profiles of ZnO and Zn-Ti-O sorbents in the temperature range 400–700°C where the resistances to reaction are due to diffusion through the product layer and the surface reaction. This model provided a more accurate description of the solids as seen in SEM micrographs than a nonoverlapping model. For Zn-Ti-O sorbents, a discrete bimodal grain size distribution was used in the model while for ZnO, a single grain size was used.

The activation energies of the product layer diffusion coefficient for ZnO and Zn-Ti-O sulfidation were similar, 26.6 + 0.3 kcal/mol. However, as the relative content of titanium in the solids increased, the pre-exponential factor decreased.

From the similarity in activation energies, it was surmised that during sulfidation of both ZnO and Zn-Ti-O, diffusion in the product layer occurs primarily through ZnS. Accordingly, diffusion through ZnS was faster than through TiO_2. TiO_2 in the product layer served to reduce the cross-sectional diffusional area and increased the tortuosity of the diffusion path. Thus, the product layer diffusion coefficient decreased as the TiO_2 content in the product layer increased.

Acknowledgment

This research was supported by the U.S. Department of Energy/University Coal Research Program under Contract No. DE-FG22-88PC88927. S. Lew appreciates useful comments and suggestions from Prof. R. M. Latanision, Dept. of Materials Science & Engineering, MIT.

Notation

A_{avg} = average surface area of plate
b = stoichiometric factor [that is, $A(g) + bB(s) \rightarrow cC(g) + dD(s)$]
C_{Ao} = concentration of reactant A (H_2S) in the bulk gas
D_e = product layer diffusion coefficient
ϵ_o = initial porosity of solid
ϵ = porosity of solid
f = grain geometric factor ($4\pi/3$ for a sphere, π/L_{avg} for a cylinder, and $2A_{avg}$ for a plate)
F_g = grain shape factor (3 for a sphere, 2 for a cylinder, and 1 for a plate)
k = rate constant
L_{avg} = average length of cylinder
$n_o(r_o)dr_o$ = number of grains per unit volume with size in the initial size range $[r_o, r_o + dr_o]$
ρ_s = concentration of reactant solid
$r_{o,max}$ = upper limit of initial grain radius
$r_{o,min}$ = lower limit of initial grain radius
r = grain radius
R = ideal gas constant
S = surface area per unit volume of solid
T = absolute temperature, K
v_i = volume fraction of component i in the product layer
$Y(t)$ = lower limit of the size range of active grains at time t
X = fractional conversion
Z = stoichiometric volume ratio of solid product to solid reactant

Subscripts

r = refers to values or properties at the reaction surface
p = refers to values or properties at the pore surface (solid reactant + product)

Literature Cited

Courty, P., H. Ajot, C. Marcilly, and B. Delmon, "Oxydes Mixtes ou en Solution Solide sous Forme Tres Divisee Obtenus per Decomposition Thermique de Precurseurs Amorphes," *Powder Tech.*, **7**, 21 (1973).

Focht, G. D., P. V. Ranade, and D. P. Harrison, "High-Temperature Desulfurization Using Zinc Ferrite: Reduction and Sulfidation Kinetics," *Chem. Eng. Sci.*, **43**(11), 3005 (1988).

Gibson, J. B., and D. P. Harrison, "The Reaction Between Hydrogen Sulfide and Spherical Pellets of Zinc Oxide," *Ind. Eng. Chem. Process Des. Dev.*, **19**, 231 (1980).

Grindley, T., and G. Steinfeld, "Development and Testing of Rege-

nerable Hot Coal Gas Desulfurization Sorbents," Final Report DOE/MC/16545-1125 (Oct. 1981).
Kingery, W. D., H. K. Bowen, and D. K. Ulmann, *Introduction to Ceramics*, 2nd ed., Wiley, New York (1976).
Lew, S., K. Jothimurugesan, and M. Flytzani-Stephanopoulos, "High Temperature H_2S Removal from Fuel Gases by Regenerable Zinc Oxide-Titanium Dioxide Sorbents," *Ind. Eng. Chem. Res.*, **28**, 535 (1989).
Lew, S., "High-Temperature Sulfidation and Reduction of Zinc Titanate and Zinc Oxide Sorbents," Ph.D. Dissertation, MIT, Cambridge, MA (1990).
Lew, S., A. F. Sarofim, and M. Flytzani-Stephanopoulos, "Mechanistic and Kinetic Studies of High Temperature Coal Gas Desulfurization Sorbents," Final Report to DOE, DOE/PC88927 (Oct., 1991).
Lew, S., A. F. Sarofim, and M. Flytzani-Stephanopoulos, "The Reduction of Zinc Titanate and Zinc Oxide Solids," *Chem. Eng. Sci.*, **47**, 1421 (1992a).
Lew, S., A. F. Sarofim, and M. Flytzani-Stephanopoulos, "The Sulfidation of Zinc Titanate and Zinc Oxide Solids," *Ind. Eng. Chem. Res.*, in press (1992b).
Lindner, B., and D. Simonsson, "Comparison of Structural Models for Gas-Solid Reactions in Porous Solids Undergoing Structural Changes," *Chem. Eng. Sci.*, **36**, 1519 (1981).
Marcilly, C., P. Courty, and B. Delmon, "Preparation of Highly Dispersed Mixed Oxides and Oxide Solid Solutions by Pyrolysis of Amorphous Organic Precursors," *J. Am. Ceram. Soc.*, **53**(1), 57 (1970).
Marqueen, T. J., D. J. Carbone, and J. Ligammari, "Coal Gasification Combined Cycle Systems—Technical Horizons," *Proc. Am. Pow. Conf.*, **48**, 235 (1986).
"Chemistry of Hot Gas Cleanup in Coal Gasification and Combustion," Final Report MERC/SP 78/2, Morgantown Energy Technology Center MERC, Hot Gas Cleanup Task Force (Feb., 1978).
Ranade, P. V., and D. P. Harrison, "The Variable Property Grain Model Applied to the Zinc Oxide-Hydrogen Sulfide Reaction," *Chem. Eng. Sci.*, **36**, 1079 (1981).
Secco, E. A., "Diffusion and Exchange of Zinc in Crystalline Zinc Sulfide," *J. Appl. Phys.*, **29**, 406 (1958).
Shannon, R. D., and C. T. Prewitt, "Effective Ionic Radii in Oxides and Fluorides," *Acta Cryst.*, **B25**, 925 (1969).
Sotirchos, S. V., and H. C. Yu, "Overlapping Grain Models for Gas-Solid Reactions with Solid Product," *Ind. Eng. Chem. Res.*, **27**, 836 (1988).
Szekely, J., J. W. Evans, and H. Y. Sohn, *Gas-Solid Reactions*, Academic Press, New York (1976).
Tamhankar, S. S., M. Bagajewicz, G. R. Gavalas, P. K. Sharma, and M. Flytzani-Stephanopoulos, "Mixed-Oxide Sorbents for High-Temperature Removal of Hydrogen Sulfide," *Ind. Eng. Chem. Process Des. Dev.*, **25**, 429 (1986).
Wakao, N., and J. M. Smith, "Diffusion in Catalyst Pellets," *Chem. Eng. Sci.*, **17**, 825 (1962).

Manuscript received April 2, 1991, and revision received Dec. 5, 1991.